Selective Synthesis of Lamellar Titania with Carboxylate Precursor and Characterization by Solid-State NMR

Oc Hee Han,*,† Younkee Paik,† Yoon Soo Moon,† Sang Kyung Lee,‡ Taek Young Kim,‡ Yoon Hee Lee,‡ and Wan In Lee*,‡

Analysis Research Division, Daegu Center, Korea Basic Science Institute, Daegu 702-701, Korea, and Department of Chemistry, Inha University, Incheon 402-751, Korea

Received December 9, 2006. Revised Manuscript Received April 16, 2007

A new means of synthesizing titania mesostructures with ammonium titanyl carboxylates in basic aqueous solution is presented. With a cetyltrimethylammonium bromide (CTAB) ionic template, a lamellar titania was synthesized from an ammonium titanyl oxalate Ti-precursor, and a hexagonally ordered mesoporous titania was synthesized from an ammonium titanyl citrate Ti-precursor. The molecular structure and dynamics of cetyltrimethylammonium (CTA) cations between the lamellar titania layers were studied by solid-state NMR. ^{13}C SP MAS, CP MAS, WISE, and DRSE spectra provided the structural and molecular dynamics information on the CTA cations between the titania layers: (1) bent conformations near the head group, (2) rotation of the methylene carbons in trans conformation about the cetyl chain axes, (3) common rapid methyl group rotation, and (4) interdigitated structures in an antiparallel fashion. The cetyl chains in CTAB are interdigitated as well; however, they are all in trans conformation without any bent. Another difference is that the CTA cations in CTAB have overall lesser mobility than those between the titania layers. The possibility was discussed that the oxalates exist as ligands to the surface Ti of the lamellar titania layers and that the CTA cations interact with the oxalates.

Introduction

Since the discovery of mesoporous silicate family (M41S) with highly organized and well-defined mesopore channels by the scientists in Mobil Research and Development Co., various mesostructures of silicates have been fabricated by means of the introduction of organic templates.[1−4] Recently, this strategy has been extended to the preparation of mesoporous structures on the basis of various transition metal oxides.[5−15] TiO_2, an oxide semiconductor with a band gap of 3.2 eV, has drawn extensive attention due to its versatile commercial applications. TiO_2 in mesoporous structures of high surface area and excellent pore-channel connectivity will be an especially promising candidate for the application to photocatalysts,[16] electrochromic devices,[17] photovoltaics,[18] host−guest chemistry,[19] luminescence devices,[20] and others. Therefore, the tailoring of TiO_2 mesostructure is considered to be one of the critical issues in the realization of these applications.

Differently from silicate mesoporous structures, however, formation of mesoporous titania is much more complicated, because the sol−gel reaction of Ti-precursor is difficult to control, and the mesopores are subject to collapse by the stress generated during the crystallization of TiO_2 grains. To this point, a limited success has been achieved in the fabrication of bulk mesoporous TiO_2,[15,21−33] and the problems

* Corresponding author. Address: Analysis Research Division, Daegu Center, Korea Basic Science Institute (KBSI), 1370 Sankyuck-dong, Book-gu, Daegu 702-701, Republic of Korea (O.H.H.). Phone: 82 53-950-7912 (O.H.H); 82 32-863-1026 (W.I.L.). Fax: 82 53-959-3405 (O.H.H.); 82 32-867-5604 (W.I.L.). E-mail: ohhan@kbsi.re.kr (O.H.H); wanin@inha.ac.kr (W.I.L.).

† Korea Basic Science Institute.

‡ Inha University.

(1) Kresge, C. T.; Leonowick, M. E.; Roth, W. J.; Vartuli, J. C.; Beck, J. S. *Nature* **1992**, *359*, 710−712.
(2) Beck, J. S.; Vartuli, J. C.; Roth, W. J.; Leonowick, M. E.; Kresge, C. T.; Schmitt, K. D.; Chu, C. T.-W.; Olson, D. H.; Sheppard, E. W.; McCullen, S. B.; Higgins, J. B.; Schlenker, J. L. *J. Am. Chem. Soc.* **1992**, *114*, 10834−10843.
(3) Zhao, D.; Feng, J.; Huo, Q.; Melosh, N.; Frederickson, G. H.; Chmelka, B. F.; Stucky, G. D. *Science* **1998**, *279*, 548−552.
(4) Tanev, P. T.; Pinnavaia, T. J. *Science* **1995**, *267*, 865.
(5) Lyu, Y.-Y.; Yi, S. H.; Shon, J. K.; Chang, S.; Pu, L. S.; Lee, S.-Y.; Yie, J. E.; Char, K.; Stucky, G. D.; Kim, J. M. *J. Am. Chem. Soc.* **2004**, *126*, 2310.
(6) Soler-Illia, G. J. A. A.; Sanchez, C.; Lebeau, B.; Patarin, J. *Chem. Rev.* **2002**, *102*, 4093.
(7) Yu, C.; Tian, B.; Zhao, D. *Curr. Opin. Solid State Mater. Sci.* **2003**, *7*, 191.
(8) Bartl, M. H.; Boettcher, S. W.; Frindell, K. L.; Stucky, G. D. *Acc. Chem. Res.* **2005**, *38*, 263.
(9) Soler-Illia, G. J. A. A.; Crepaldi, E. L.; Grosso, D.; Sanchez, C. *Curr. Opin. Colloid Interface Sci.* **2003**, *8*, 109.
(10) Patarin, J.; Lebeau, B.; Zana, R. *Curr. Opin. Colloid Interface Sci.* **2002**, *7*, 107.
(11) Antonelli, D. M.; Ying, J. Y. *Chem. Mater.* **1996**, *8*, 874.
(12) Bagshaw, S. A.; Pinnavaia, T. J. *Angew. Chem., Int. Ed.* **1996**, *35*, 1102.
(13) Ciesla, U.; Schacht, S.; Stucky, G. D.; Unger, K. K.; SchuÈth, F. *Angew. Chem., Int. Ed.* **1996**, *35*, 541.
(14) Liu, P.; Liu, J.; Sayari, A. *Chem. Commun*. **1997**, 557.
(15) Yang, P.; Zhao, D.; Margolese, D. I.; Chmelka, B. F.; Stucky, G. D. *Nature* **1998**, *396*, 152. Yang, P.; Zhao, D.; Margolese, D. I.; Chmelka, B. F.; Stucky, G. D. *Chem. Mater.* **1999**, *11*, 2813.
(16) Yu, J. C.; Wang, X. C.; Fu, X. Z. *Chem. Mater.* **2004**, *16*, 1523.
(17) Choi, S. Y.; Mamak, M.; Coombs, N.; Chopra, N.; Ozin, G. A. *Nano Lett.* **2004**, *4*, 1231.
(18) Vogel, R.; Meredith, P.; Kartini, I.; Harvey, M.; Riches, J. D.; Bishop, A.; Heckenberg, N.; Trau, M.; Rubinsztein-Dunlop, H. *Chem. Phys. Chem.* **2003**, *4*, 595.
(19) Perez, M. D.; Otal, E.; Bilmes, S. A.; Soler-Illia, G. J. A. A.; Crepaldi, E. L.; Grosso, D.; Sanchez, C. *Langmuir* **2004**, *20*, 6879.
(20) Frindell, K. L.; Bartl, M. H.; Popitsch, A.; Stucky, G. D. *Angew. Chem., Int. Ed.* **2002**, *41*, 959.
(21) Antonelli, D. M.; Ying, J. Y. *Angew. Chem., Int. Ed.* **1995**, *34*, 2014.
(22) Antonelli, D. M. *Microporous Mesoporous Mater.* **1999**, *30*, 315.

10.1021/cm062916w CCC: $37.00
Published on Web 06/27/2007

encountered in the formation of robust mesostructure and control of mesophase remain to be solved.

Lamellar titania draws comparatively less attention from the scientific community, because the layered super structure automatically collapses after the removal of the organic template and its structural regularity is not sufficient. However, if the lamellar titania can be fabricated in the form of highly ordered layered structure with a robust sheet framework, it will have a potential application as a new material for intercalation or host−guest chemistry. So far, there have been only a few reports on the preparation of lamellar titania, which have been derived from titanium alkoxides and cationic surfactants as Ti-precursor and organic templates, respectively.[34−38] When the cationic surfactants such as cetyltimethylammonium bromide (CTAB) are used as organic templates, a basic environment is required during the synthetic reaction in order to promote an electrostatic interaction between the self-assembled cationic surfactant and the inorganic sol. Typical Ti-precursors such as titanium alkoxide or titanium alkoxy-β-diketonate can be stabilized in an acidic condition, but they are quickly hydrolyzed and precipitated under basic conditions. Therefore, the stabilization of Ti-precursors in basic solution is very important, and the selection of appropriate Ti-precursors will be essential to the successful control of titania mesostructures.

Herein, we report a new route to controlling titania mesostructures by applying the ammonium titanyl carboxylates, which has never been used in the preparation of mesoporous structures. A highly ordered lamella titania and a hexagonally ordered mesoporous titania were prepared and the structures and dynamics of the intercalated cetyltrimethylammonium (CTA) cations in the lamellar titania was studied in depth by solid-state NMR, which has been powerful in probing molecular structure and dynamics of molecules with a long linear alkyl chain.[39−46] The long linear alkyl chains in the crystalline phases are almost all in trans conformations, and the chemical shifts of the inner methylene carbons range between 34.2 and 32.8 ppm according to their motional state and molecular packing.[39] The solid-state NMR study on the CTA cations in MCM-41 revealed that the surfactants in the pores had a high content of gauche conformations and the anisotropic motions were progressively reduced from the chain end toward the polar head.[40] The CTA cations in the ordered mesophase silicate were less mobile than those in the disordered silicate.[41] In the mesopores, the methylene groups near the trimethylammonium head groups manifested less motion than those farther away from the head groups and the methyl groups belonging to the head groups showed the splitting and /or shifts of the resonance frequencies.[2,40,41] All of these observations suggest that the inner surface of the mesopores interact more strongly with the polar head groups of the surfactants than with the rest of the surfactants.[2,40,41] The conformation and mobility of surfactant molecules intercalated into clay[42] and of self-assembled monolayers on oxide surfaces[43,44] were also studied by solid-state NMR. When the clay with 22 Å spacing between the layers was fully ion exchanged with the surfactant cations, ordered all-trans conformation was more typical than disordered trans-gauche mixture conformation.[42] In contrast, when the clay with 7 Å spacing was partially ion exchanged with the surfactant cations, the disordered conformation was more populated.[42] The molecules in the ordered conformation were as rigid as in crystalline materials, whereas those in the disordered conformation were similar to those in liquid crystalline.[42] Upon heating, the surfactant molecules in the ordered conformation became disordered, whereas the molecules in the disordered conformation remained more or less unchanged.[42] However, it has been confirmed not only in the long linear alkyl chains in the crystalline phases[39,45] but also in the self-assembled monolayers[43] that all trans conformation does not necessarily entail rigid molecules as in crystalline materials. Molecules in all trans conformation can rotate fast about the molecular axes in a certain condition.[39,43,45]

Experimental Section

In the preparation of mesoporous titania in hexagonal ordering, ammonium titanyl citrate (ATC) was used as the Ti-precursor. Methylamine (Aldrich, 98+%) was used to maintain a basic environment during the cationic surfactant-assisted sol−gel reaction. Other amines such as diethylamine or trimethylamine can also be used for this purpose. A total of 0.41 mmol of CTAB and 3.40 mmol of methylamine were dissolved in a stoichiometric amount of water by stirring at 40 °C. A total of 2.56 mmol of ATC in other water was then added to the first solution dropwise. A white precipitation initially formed and was soon dissolved to form a transparent solution with the further addition of the ATC aqueous solution. The final molar ratio of ATC, CTAB, methylamine, and water in the solution, producing a mesoporous structure, was 1.00: 0.16:1.33:125−250. This clear solution was then transferred to a glass-lined autoclave and reacted for 3−4 days at 100 °C. The prepared mesoporous titania was washed with ethanol and water, and dried in a vacuum at room temperature. To remove the CTAB, the as-prepared sample was gently washed several times with 0.1 M HCl ethanol/water solution. The remnant CTAB was then photocatalytically removed by the irradiation of light in the

(23) Wang, Y.; Tang, X.; Yin, L.; Huang, W.; Hacohen, Y. R.; Gedanken, A. *Adv. Mater.* **2000**, *12*, 1183.
(24) Yoshitake, H.; Sugihara, T.; Tatsumi, T. *Chem. Mater.* **2002**, *14*, 1023.
(25) Sayari, A.; Liu, P. *Microporous Mater.* **1997**, *12*, 149.
(26) Ulagappan, N.; Rao, C. N. R. *Chem. Commun.* **1996**, 1685.
(27) Yue, Y.; Gao, Z. *Chem. Commun.* **2000**, 1755.
(28) Peng, Z.; Shi, Z.; Liu, M. *Chem. Commun.* **2000**, 2125.
(29) Yu, J. C.; Zhang, L.; Yu, J. *New J. Chem.* **2002**, *26*, 416.
(30) Tian, B.; Yang, H.; Liu, X.; Xie, S.; Yu, C.; Fan, J.; Tu, B.; Zhao, D. *Chem. Commun.* **2002**, 1824.
(31) Luo, H.; Wang, C.; Yan, Y. *Chem. Mater.* **2003**, *15*, 3842.
(32) Stone, V. F.; Davis, R. J. *Chem. Mater.* **1998**, *10*, 1468.
(33) Yang, P.; Zhao, D.; Margolese, D. I.; Chmelka, B. F.; Stucky, G. D. *Chem. Mater.* **1999**, *11*, 2813.
(34) Fujii, H.; Ohtaki, M.; Eguchi, K. *J. Am. Chem. Soc.* **1998**, *120*, 6832.
(35) On, D. T. *Langmuir* **1999**, *15*, 8561.
(36) Putnam, R. L.; Nakagawa, N.; McGrath, K. M.; Yao, N.; Aksay, I. A.; Gruner, S. M.; Navrotsky, A. *Chem. Mater.* **1997**, *9*, 2690.
(37) Lin, W.; Pang, W.; Sun, J.; Shen, J. *J. Mater. Chem.* **1999**, *9*, 641.
(38) Bai, N.; Li, S.; Chen, H.; Pang, W. *J. Mater. Chem.* **2001**, *11*, 3099.
(39) Ishikawa, S.; Kuroso, H.; Ando, I. *J. Mol. Struct.* **1991**, *248*, 361.
(40) Simonutti, R.; Comotti, A.; Bracco, S.; Sozzani, P. *Chem. Mater.* **2001**, *13*, 771.
(41) Wang, L.-Q.; Liu, J.; Exarhos, G. J.; Bunker, B. C. *Langmuir* **1996**, *12*, 2663.
(42) Wang, L.-Q.; Liu, J.; Exarhos, G. J.; Flanigan, K.Y.; Bordia, R. *J. Phys. Chem. B* **2000**, *104*, 2810 and references therein.
(43) Gao, W.; Reven, L. *Langmuir* **1995**, *11*, 1860.
(44) Gao, W.; Dickinson, L.; Grozinger, C.; Morin, F. G.; Reven, L. *Langmuir* **1996**, *12*, 6429.
(45) Möller, M.; Cantow, H. J.; Drotoll, H.; Emeis, D.; Lee, K. S.; Wegner, G. *Makromol. Chem.* **1986**, *187*, 1237.
(46) VanderHart, D. L. *J. Magn. Reson.* **1981**, *44*, 117.

wavelength of 350 nm. The photocatalytic reaction was performed for a long period (5−7 days) under low-intensity UV irradiation with a 12 W a homemade lamp assembled with commercial photodiodes, because the collapse of mesopore can be minimized by slow decomposition of organic templates.

As a Ti-precursor for the preparation of the lamellar titania, ammonium titanyl oxalate (ATO; Aldrich, 98%) instead of ATC was introduced. The final molar ratio of ATO, CTAB, methyl amine, and water in the solution was 1.00:0.16:1.33:140. This clear solution was reacted in a glass-lined autoclave for 2 days at 110 °C.

X-ray diffraction (XRD) patterns were obtained by using a Multiflex diffractometer (Rigaku Co., Japan) with monochromated high-intensity Cu Kα radiation. The TEM images were obtained with a S-4500 transmission electron microscope (Hitachi Ltd., Japan) operated at 250 kV. The samples were gently dispersed in methanol, and the suspension was dropped on a holey amorphous carbon film deposited on a Ni grid (JEOL Ltd., Japan). The XPS spectra were recorded by Sigma Probe Instrument (Thermo VG, U.K.) equipped with a standard monochromatic Al Kα excitation source ($h\nu = 1486.6$ eV). The binding energy scale was calibrated by measuring the C 1s peak at 284.5 eV from the surface contamination.

All NMR spectra were acquired using an AVANCE II 400 MHz NMR instrument (Bruker Biospin Co., Germany) with a cross polarization (CP) MAS probe for 4 mm rotors at room temperature. ^{13}C single-pulse magic angle spinning (SP MAS) spectra were obtained under proton decoupling with a 30° pulse, a pulse repetition delay of 20 s, a spectral width of 100 kHz, and a spinning rate of 10 kHz. ^{15}N CP MAS spectra were acquired with a contact time of 4 ms, a repetition delay time of 1 s, a spectral width of 50 kHz, and a sample spinning rate of 5 kHz. The pulse length for a 90° flip angle was 3 μs for all ^{13}C, ^{15}N, and ^{1}H. The ^{13}C and ^{15}N chemical shifts were referenced to tetramethylsilane (0 ppm) and [^{15}N] glycine (11.59 ppm),[47] respectively.

Two-dimensional (2D) wide-line separation (WISE)[48,49] spectra were acquired with a delay increment of 0.5 μs starting from 0.5 μs between a proton 90° pulse and a CP pulse. A contact time of 150 μs for CP and a spinning rate of 4.5 kHz were used. The spectral width in the ^{13}C domain was set to 100 kHz.

Dipolar rotational spin echo (DRSE) ^{13}C{^{1}H} experiments were performed by varying the number of semi-windowless MREV-8 cycles in the dipolar time dimension (t_1) applied during the second rotor period.[50,51] The evolution of ^{13}C magnetization due to chemical shift effects was refocused after two rotor periods by a ^{13}C 180° pulse applied after the first rotor period.[50,51] The spinning rate was chosen so that 16 MREV-8 cycles with a cycle time of $t_c = 24$ μs exactly fit within one rotor period ($T_r = 384$ μs). A 16-point discrete Fourier transform was performed to obtain the dipolar frequency spectrum.

Results and Discussion

When ATC with a relatively bulkier ligand citrate was used as a Ti-precursor in the preparation of mesoscopic titania, the as-prepared sample was a hexagonally ordered mesoporous titania, as shown in Figure 1a. The molar ratio of H_2O to ATC in the reaction solution was 217. A similar mesoporous titania structure was also formed at the molar ratio of 140.

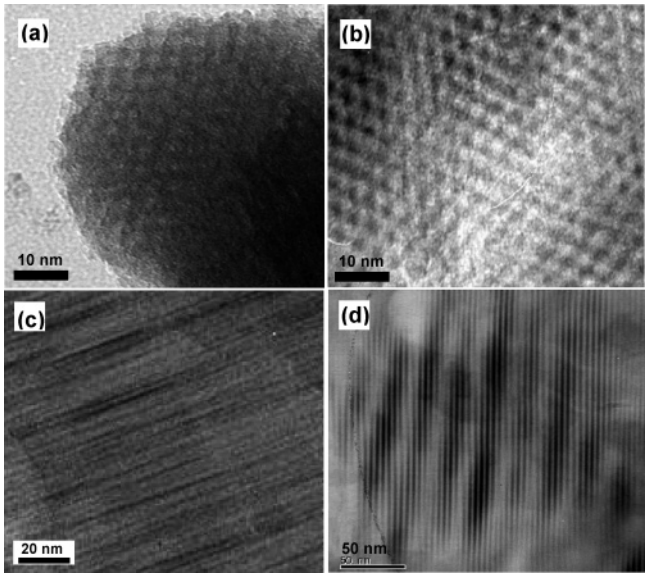

Figure 1. TEM images for mesoporous and lamellar titania samples. (a) Hexagonal mesoporous titania containing CTA template and (b) that after template removal by photocatalytic decomposition. (c) Typical lamellar titania and (d) the moirés pattern found for the superimposed lamellar titania structure.

In this TEM image, the CTAB used as an organic template occupies the mesopores. When this mesoporous titania was annealed at 400 °C to remove the surfactant, the corresponding structure completely collapsed. However, the surfactant could be successfully removed, without destroying the mesoporous structure by a photocatalytic decomposition method, as shown in Figure 1b. Figure 2a shows the XRD patterns for the as-prepared and the surfactant-removed mesoporous TiO_2. After the removal of the CTAB, the long-range ordering of the mesopore appreciably deteriorated. In the XRD pattern of the as-prepared mesoporous TiO_2, the strong (100) peak at 2.08° indicates that the pore-to-pore distance ($(2/\sqrt{3})d_{100}$) is 4.90 nm, which is compatible with that estimated from the TEM image.

When ATO was used as a Ti-precursor, the as-prepared sample had a lamellar titania structure with an interlayer distance of about 2.6 nm as indicated by the TEM image in Figure 1c. The thickness of the titania layer estimated was 0.8−1.0 nm, whereas the interlayer gap was about 1.6−1.8 nm. However, the determination of exact values by TEM remains unfeasible, because the incurred electron-beam damage makes high-resolution TEM imaging of the lamellar titania with a high organic composition technically impossible. The sharp and intense (001) and (002) diffraction peaks shown in the XRD pattern in Figure 2b indicate that the prepared titania is a highly ordered lamellar structure. The interlayer distance determined from the peak positions is 2.58 nm, which corresponds to the TEM image.

In a certain area of lamellar titania, highly organized fringes were observed over a wide range, as shown in the TEM image of Figure 1d. The distance between the fringes

(47) Shoji, A.; Ozaki, T.; Fujito, T.; Deguchi, K.; Ando, I.; Magoshi, J. *J. Mol. Struct.* **1998**, *441*, 251.
(48) Schmidt-Rohr, K.; Clauss, J.; Spiess, H. W. *Macromolecules* **1992**, *25*, 3273.
(49) Clauss, J.; Schmidt-Rohr, K.; Adam, A.; Boeffel, C.; Spiess, H. W. *Macromolecules* **1992**, *25*, 5208.
(50) Schaefer, J.; McKay, R. A.; Stejskal, E. O. *J. Magn. Res.* **1983**, *52*, 123.
(51) Schaefer, J.; McKay, R. A.; Stejskal, E. O. *Macromolecules* **1984**, *17*, 1479.

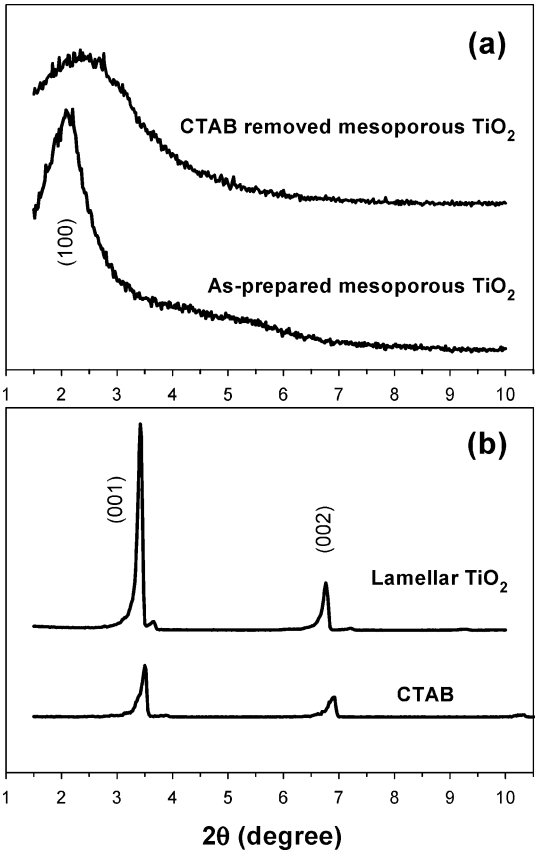

Figure 2. Small-angle XRD patterns for (a) mesoporous titania samples as-prepared and surfactant-removed and (b) lamellar titania and CTAB.

was about 5.1 nm, which was appreciably longer than the interlayer distance. We believe that those fringes formed a kind of moiré pattern due to the overlap of two individual lamellar titania domains. Such patterns are often observed in the TEM analyses when highly crystallized ultrathin samples in slightly different crystal orientations are superimposed on each other. Thus, the lamellar titania synthesized in this work similarly has a highly organized super-structure over a large area.

This highly organized lamellar titania structure was formed only at a specific composition of reactants. The appropriate molar ratio of ATO to CTAB was 0.15−0.17, and the water content was 135−150 equiv. When reactant compositions varied, mixed lamellar or less-organized phases were usually formed. The synthetic window of the mesoporous titania in hexagonal array seems to be relatively wider than that of the lamellar structure. The molar ratio of ATC to CTAB was 0.10−0.25, and the water content was 125−250 equiv.

The surfactant organization in amphiphilic liquid-crystal arrays is described in terms of the surfactant packing parameter, so-called *g*-factor ($g = V/(a_0 l)$, where V is the total volume of the surfactant chains plus any cosolvent organic molecules between the chains, a_0 is the effective head group area at the micelle surface, and l is the kinetic surfactant tail length.).[52,53] The *g*-factor is conveniently used as a key parameter in determining the mesophase. For example, lamellar structures can be formed at a relatively

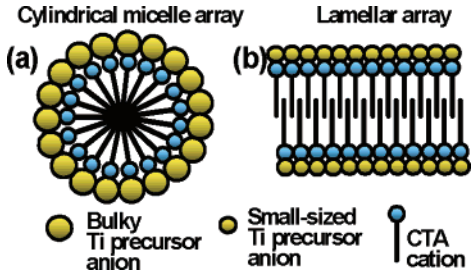

Figure 3. Schematic diagrams of proposed arrays of CTA cations formed with (a) bulky Ti-precursor anions and (b) small-sized Ti-precursor anions.

high *g*-factor such as $g > 2/3$, whereas hexagonal and cubic (*Ia*3*d*) mesophases can be obtained at around 1/2 and 1/2−2/3, respectively. Usually, the phases of mesoporous structures are controlled by varying the surfactant concentration, the molar ratio of metal precursor to surfactant, and/or by adding of cosolvent. In the present work, we demonstrate that the functional group of the Ti-precursor can also play a key role in determining the mesophase of titania. When ATC containing the relatively bulky ligand citrate was applied to the synthesis, a hexagonally ordered mesoporous titania was obtained, whereas the application of ATO with the small-sized ligand oxalate led to a lamellar structure. We deduce that this result originates from the strong ionic interaction between CTAB and the Ti-precursor. In the basic aqueous condition, the ammonium titanyl carboxylate produces the titanium carboxylate anion, and the cationic CTA and the anionic titanyl carboxylate will then form a stable ionic pair. Presumably, this strong Coulomb interaction would affect the cylindrical micelle array of CTA cations. In this circumstance, the size of anionic titanyl carboxylates would be an important factor in determining the self-assembly of CTA cations in aqueous solution. As suggested in the Figure 3 diagram, if the size of titanyl carboxylates bound to CTA cations is sufficiently large, they can form an intermolecular interaction between the neighboring titanyl carboxylates without disturbing the cylindrical array of CTA cations. On the other hand, when the size of Ti-precursor is similar to or smaller than the head group size of a CTA cation, the Ti-precursor cannot interact with the neighboring precursors without disturbing the cylindrical micelle array of CTA cations. In this circumstance, the lamellar structure would be a more appropriate way of array, as suggested in Figure 3b. What we observed here is a typical example of a cooperative interaction between the surfactant and the precursor. Accordingly, the bulkiness of metal precursors can also be an important factor in determining mesoporous structure when the surfactant and metal precursor strongly interact.

A notable observation of the prepared lamellar titania is that the interlayer *d*-spacing (2.58 nm) is very close to that of the naked CTAB itself, as shown in the XRD patterns of Figure 2b. The CTAB samples are known to also form a lamellar array with an interlayer distance of 2.54 nm.[54] However, the intensity of the diffraction patterns for the lamellar titania is much stronger than that for the pure CTAB. In addition, the lamellar titania presented clear TEM images,

(52) Huo, Q.; Margolese, D. I.; Stucky, G. D. *Chem. Mater.* **1996**, *8*, 1147.
(53) Gallis, K. W.; Landry, C. C. *Chem. Mater.* **1997**, *9*, 2035.
(54) Campanelli, A. R.; Scaramuzza, L. *Acta. Crystallogr., Sect. C* **1986**, *42*, 1380.

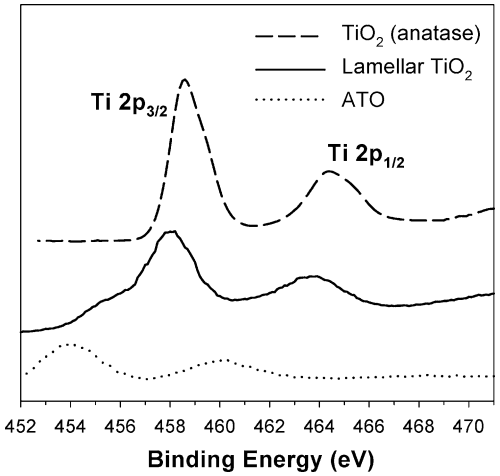

Figure 4. High-resolution XPS of Ti 2p for 15 nm anatase TiO_2 nanoparticles, as-prepared lamellar titania, and ATO Ti-precursor.

indicating a layered structure, whereas an appreciably clear image could not be obtained from the pure CTAB. The absence of any XRD patterns in the range of 20−30° indicates the absence of the bulk TiO_2 crystalline phase in the lamellar titania structure.

Figure 4 shows the high-resolution X-ray photoelectron spectra of Ti 2p for the 15 nm anatase TiO_2 nanoparticles,[55] the as-prepared lamellar titania, and the ATO Ti-precursor. The binding energies of Ti $2p_{3/2}$ were 458.6, 458.2, and 454.2 eV, respectively. The Ti binding energy of lamellar titania was only slightly lower than that of the anatase particles, but considerably higher than that of ATO. This suggests that the majority of Ti in the titania layer is Ti^{4+}, which exists as a form of TiO_2. A broad shoulder peak on the lower energy side of Ti $2p_{3/2}$ for the lamellar titania implies that some of the Ti is in a lower oxidation state. Presumably, the Ti located on the surface of titania block is in the low oxidation state. There is a possibility that some of the oxalate ligands are still present on the surface of the titania layer.

To estimate the content of the inorganic in the lamellar titania, we calcined 0.13 g of the as-prepared sample at 550 °C in a nitrogen environment for 1 h and subsequently in air for 4 h, and weighed the residual TiO_2 ash. From this gravimetric analysis, TiO_2 turned out to comprise 31 ± 5 wt % as-prepared lamellar titania. From the TEM image and the gravimetric analysis, the thickness of the titania layer was estimated to be 0.8−1.0 nm. Thus the space available for CTA cations between the lamellar titania is only 1.6−1.8 nm, which is even shorter than the full length of a CTA cation in trans conformation (∼2 nm). If the cetyl chains are interdigitated, the space between the lamellar titania should be considerably larger than 2 nm, unless the cetyl chains are far from the all trans conformation. This led us to employ solid-state NMR techniques to probe the molecular structure and dynamics of the CTA cations between the titania layers.

^{13}C SP MAS spectra along with the peak assignment of the CTAB and the CTA cations between the titania layers are shown in Figure 5 and the observed chemical shifts are

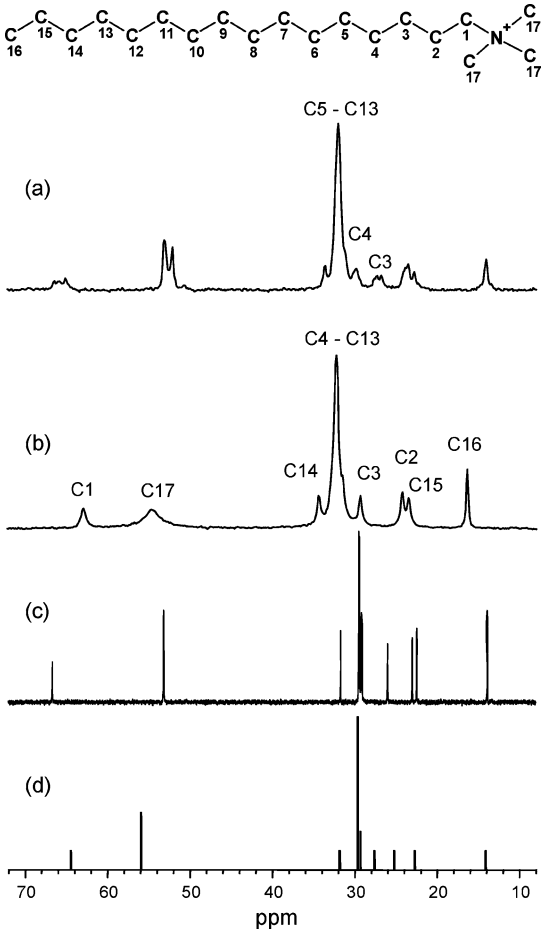

Figure 5. ^{13}C SP MAS NMR spectra of (a) CTA cations between lamellar titania layers and (b) CTAB. ^{13}C NMR spectra of (c) CTAB solution in $CDCl_3$, and (d) CTAB in gas phase simulated with the ChemDraw program.

Table 1. Peak Assignments of ^{13}C SP MAS Spectra and Chemical Shifts in parts per million

	carbon number								
	C1	C2	C3	C4	C5−C13	C14	C15	C16	C17
CTA cations	66.1	24.5	27.8	30.9	33.0	34.6	23.8	15.0	50.7
between	66.9	24.8	28.3						53.1
titania layers	67.5	25.1	28.6						54.1
CTAB	62.9	24.2	29.2	32.2	32.2	34.3	23.4	16.3	54.6
chemical shift	3.2	0.3	−1.4	−1.3	0.8	0.3	0.4	−1.3	−3.9
difference	4.0	0.6	−0.9						−1.5
	4.6	0.9	−0.6						−0.5

summarized in Table 1. The chemical shift were assigned for CTAB by comparison to the solution spectrum[40,41] in Figure 5c and the gas-phase spectrum shown in graph d in Figure 5, respectively. The gas-phase spectrum was obtained by simulation using the ChemDraw program and had the same order of the individual carbon resonance positions with the solution NMR spectrum. The chemical shifts of the CTA cations in gas phase are mainly determined according to magnetic susceptibility at each carbon as well as the time-averaged populations of trans and gauche conformations of individual carbons, whereas the chemical shifts of the CTA cations in solution are additionally influenced by solvent. Hence, unless there is a drastic difference of the conformations, the spectra obtained from the solution state or in gas phase are expected to have the same order of peak positions. This applies also to the spectrum of the crystalline CTAB.

(55) Chae, S. Y.; Park, M. K.; Lee, S. K.; Kim, T. Y.; Kim, S. K.; Lee, W. I. *Chem. Mater.* **2003**, *15*, 3326.

Relative peak intensities of the peak assignments in the SP MAS of CTAB were also confirmed. The crystal structure of CTAB shows that the cetyl chains are all in trans conformation and are arranged in an antiparallel interdigitation fashion.[54] The interdigitated bilayers of the CTA cations are stabilized by the hydrophobic interaction between cetyl chains and by the ionic interaction between trimethylammonium cations and counter anions. Our peak assignments for CTAB agree with those of ref 41 in terms of the order of peak positions but disagree with ref 40 for those of C2 and C3. This difference originates from the different peak assignments for the solution spectra. To confirm our peak assignments for the solution spectrum, we determined carbon connectivity experimentally. The CTA cations in CTAB and between the titania layers have different counter anionic species: bromine and surface oxygens of titania, respectively. Thus it was expected that the middle methylene carbons would have similar chemical shifts in both samples but the head and tail carbons would not. In fact, the inner methylene carbons, C5−C15, had similar chemical shifts for the CTA cations between the titania layers and in CTAB, whereas C1−C4, C16, and C17 exhibited relatively large chemical shift differences and C1 the largest. The small chemical shift differences of C5−C15 between the two samples suggest that the cetyl chains of the CTA cations between the titania layers are interdigitated, as in CTAB, from C5 to C15 and that C15 is located close to C5 of the neighbor chains. The interchain distances could be a little greater in the lamellar titania samples.[56] Indeed, the chemical shift 33.0 ppm for C5−C13 of the CTA cations between the titania layers was in good agreement with the reported values for the trans conformation of the inner methylene of the cetyl chains intercalated to inorganic materials.[42] C3 and C4 exhibited −1.0 and −1.3 ppm shifts on average compared with corresponding carbons of CTAB, indicating different conformations from the all-trans conformation. C2 showed downfield shifts of ∼0.6 ppm on average, due to the combined effect from conformational, anionic, and spatial changes. C16's −1.3 ppm shift difference mainly arises from the anionic difference. The chemical shift of C1 was most drastically changed and split into three different values by intercalation to the titania layers, implying that the C1 carbons are in three different environments. Likewise, the methyl carbons bonded to the nitrogen, C17, were upfield shifted from corresponding methyl carbon peaks of CTAB and split into three peaks. These three peaks do not need to have an equal intensity in the ^{13}C SP MAS spectra, because some of the methyl groups are farther away from or closer to titania layers than the other methyl groups and range in structural heterogeneity according to the distance from the titania layer, as schematically shown in Figure 6. In our case, the resonance frequencies of the methyl carbons happened to be grouped to three peaks but with different intensities. As shown in Figure 6, some of the methyl groups and a methylene of C1 are closer to the titania layers. The three different local environment of C1 of the CTA cations between the titania layers likely reflect the three different

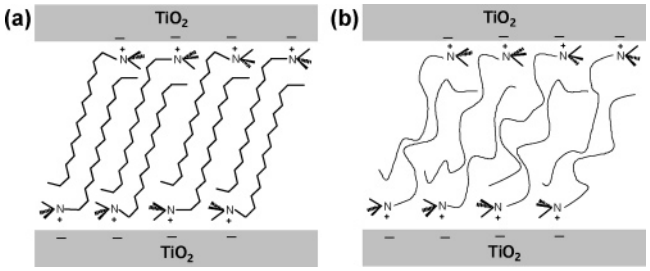

Figure 6. Schematic of the CTA cation structures between titania layers (a) with a large extent of trans conformations and (b) in the amorphous state.

locations of the methyl groups of the head group against the C1 position. In this arrangement, even in the presence of ubiquitous rapid rotation of the methyl groups, all of the methyl groups cannot be in an identical environment unless the trimethylammonium groups themselves rotate sufficiently fast. In addition, the cetyl chains between the titania layers need to be bent to be stabilized by hydrophobic interactions between the cetyl chains. Bent structures of intercalated molecules are not new.[57]

Both ^{15}N CP MAS spectra in Figure S1 of the Supporting Information for the CTA cations between the lamellar titania layers and for CTAB, have only sharp single peaks, indicating single structural phases for the CTA cations between the lamellar titania layers as well as for CTAB. The difference of the ^{15}N chemical shifts (27.4 and 30.7 ppm for the CTA cations in the lamellar titania and the CTAB, respectively) primarily reflects the anionic difference. In summary, the average structure of the CTA cations between the titania layers were similar to those in Figure 6a. Overall the long axes of the cetyl chains formed about 60° tilt angles with respect to the titania layers, resulting in a length of about ∼1.8 nm for an interdigitated CTA bilayer. This length is very close to what we measured by XRD.

However, an alternative explanation is possible, which is that the cetyl chains between the titania layers are very mobile, resulting in an amorphous structure on average, although the head group regions are relatively less mobile and anchored to the titania surface, as schematically drawn in Figure 6b. Even in this case, the titania layers can maintain a regular distance between the layers due to the balanced interactions of hydrophobic forces of cetyl chains, the charge repulsion between negatively charged titania layers, the charge repulsion between positively charged ammonium groups anchored on opposite titania surfaces, and the attraction force between the positively charged and the negatively charged species. However, the model schematically drawn in Figure 6b does not agree with the observed ^{13}C chemical shift data, indicating trans conformations for C5−C15. The model consistent with the ^{13}C chemical shift data would be that shown in Figure 6a. This is in contrast with the previous report of a large extent of gauche conformation of the CTA cations in MCM-41 mesopores.[40]

From a comparison of the SP MAS and the CP MAS spectra of CTAB and the CTA cations between the titania layers shown in Figure S2, some molecular dynamics

(56) Lee, Y.; Choi, J.; Choi, Y.-W.; Sohn, D. *J. Phys. Chem. B* **2003**, *107*, 12374 and references therein.

(57) Kaneno, M.; Yamaguchi, S.; Nakayama, H.; Miyakubo, K.; Ueda, T.; Eguchi, T.; Nakamura, N. *Int. J. Inorg. Mater.* **1999**, *1*, 379.

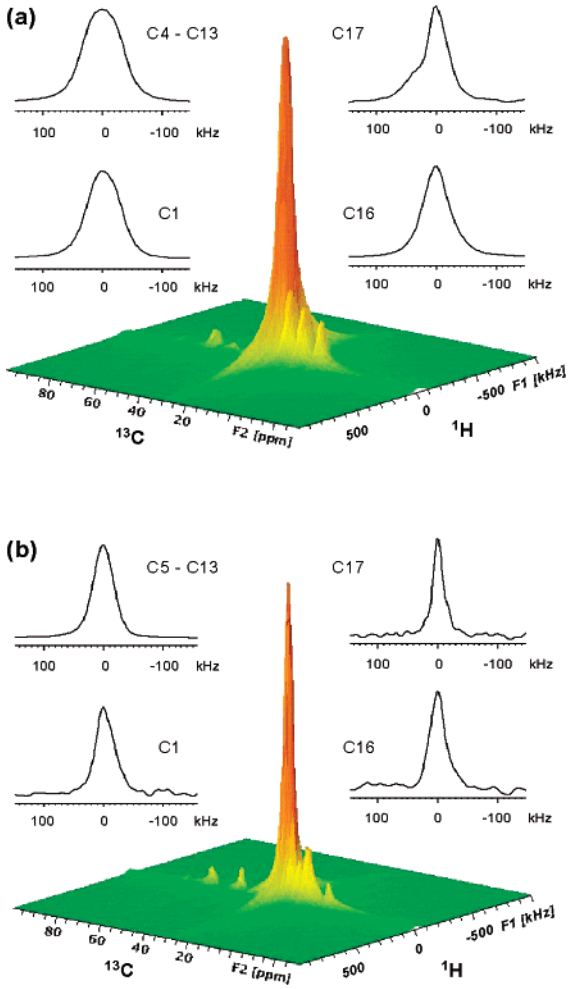

Figure 7. Two-dimensional WISE NMR spectra and slices in the ^{1}H dimension of (a) CTAB and (b) the CTA cations in titania layers. The 2D spectra are displayed in magnitude mode and the ^{1}H slices are in pure absorption mode.

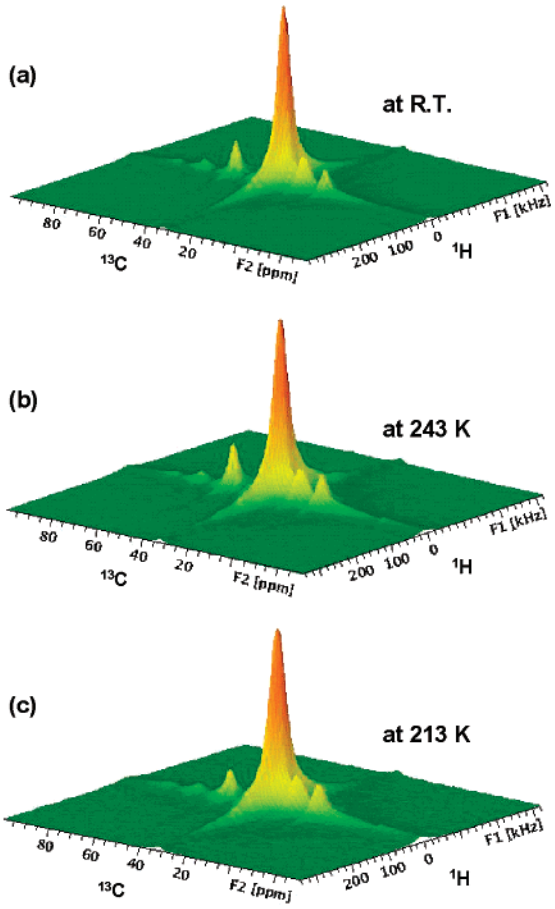

Figure 8. Two-dimensional WISE spectra of CTA cations in titania layers at (a) room temperature, (b) 243 K, and (c) 213 K.

information can be obtained. No noticeable difference was observed between the SP MAS and the CP MAS spectra except the fact that the signal intensity of methyl peaks were significantly reduced in the CP MAS spectra. Because CP tends to enhance the signal from the rigid, the signal from rotating methyl groups is relatively reduced. In contrast with the previous report on the long alkyl chains in MCM-41,[40] clay,[42] or self-assembled monolayers,[43] the linewidths and chemical shifts of the peaks in our MAS spectra taken at low temperatures as low as 213 K (not shown) were not appreciably changed.

Thus, to study the dynamic properties of the CTA cations between the titania layers in further detail, we carried out WISE experiments. Figure 7 shows the 2D WISE NMR spectra of CTAB and the CTA cations between the titania layers. Slices in the ^{1}H dimension for some selected carbons are also displayed for comparison of molecular dynamics of individual carbon peaks. The ^{1}H linewidths of the CTA cations between the titania layers (Figure 7b) are generally narrower, by about 20 kHz, than the corresponding linewidths of CTAB (Figure 7a). This indicates that the CTA cations between the titania layers have smaller intrinsic ^{1}H−^{1}H dipolar coupling or undergo more molecular motions than CTAB, which reduces the ^{1}H−^{1}H dipolar interactions and results in the narrower ^{1}H linewidths. The 2D WISE spectra at different temperatures (Figure 8) confirm that more molecular motion is the reason for the narrower linewidths of the CTA cations between the titania layers. When the sample temperature of the CTA cations between the titania layers was lowered to 213 K, the ^{1}H linewidths of individual carbon sites became broader and more similar to those of CTAB at room temperature.

The linewidths of methylene carbons, C1−C15, are much broader than those of methyl carbons, C16 and C17 (for comparison, sliced spectra for some selected carbons, i.e., C1, C5−13, C16, and C17 are shown in Figure 7). This is due to the rapid methyl group rotation,[49] which effectively decouples the ^{1}H−^{1}H dipolar interactions, resulting in narrower ^{1}H linewidths. The following linewidth differences among the methylene carbons were observed: the ^{1}H linewidths of C1s are smaller by about 5−10 kHz than those of C5−C13 in both CTAB and the CTA cations between the titania layers. However, 2D WISE is usually employed in comparing the molecular dynamics of different domains or systems.[48,49] The small difference of 5−10 kHz between the C1 and C5−C13 within the same molecule might arise from the differing intrinsic ^{1}H−^{1}H dipolar coupling environments of individual carbon sites rather than from real molecular motional difference. Therefore, a separated local field (SLF) method was used to probe the molecular dynamics of the individual carbon sites not influenced by an inherent ^{1}H−^{1}H dipolar coupling difference.

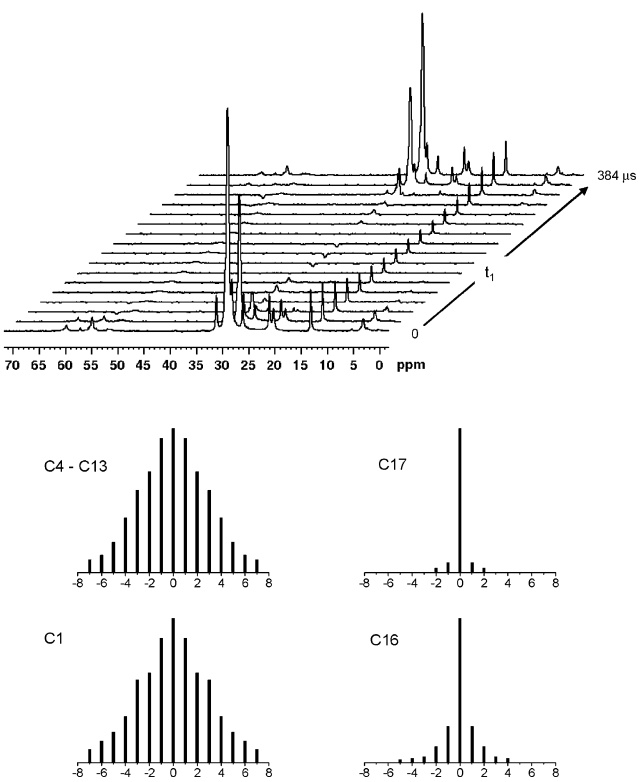

Figure 9. Dipolar rotational spin−echo ^{13}C NMR spectra of CTAB (upper) and dipolar patterns obtained by 16-point discrete Fourier transform of signal evolutions in t_1-dimension for selected carbons (lower).

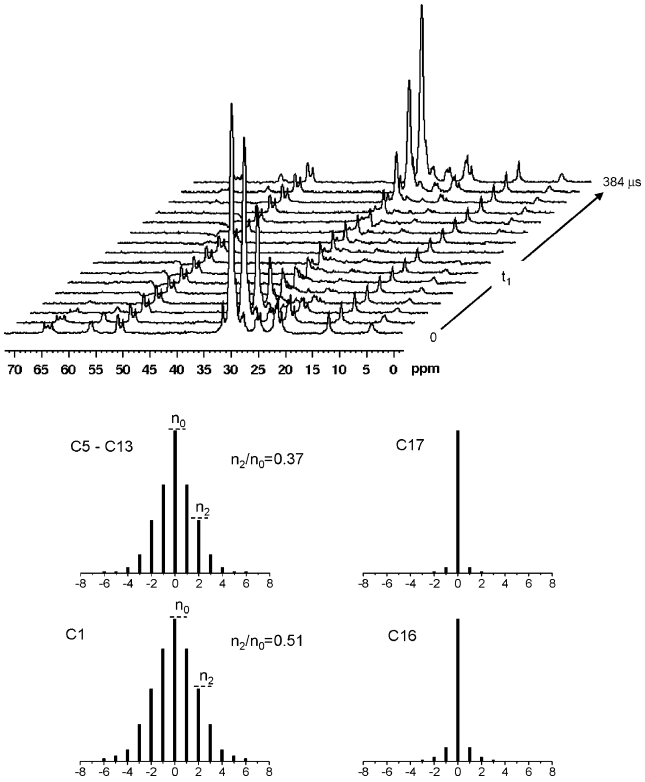

Figure 10. Dipolar rotational spin−echo ^{13}C NMR spectra of CTA cations between titania layers (upper) and dipolar patterns obtained by 16-point discrete Fourier transform of signal evolutions in t_1-dimension for selected carbons (lower).

Figures 9 and 10 show the DRSE spectra of CTAB and the CTA cations between the titania layers, respectively. The individual ^{13}C signals were modulated because of $^{13}C-^{1}H$ heteronuclear dipolar interactions along the t_1-dimension and refocused after one rotor period ($T_r = 384$ μs) by MAS, whereas the effects of the strong $^{1}H-^{1}H$ couplings were removed by MREV-8 cycles.[50,51] However, in practice, the $^{1}H-^{1}H$ decoupling by a multiple-pulse sequence such as MREV-8 or WAHUHA cycles is incomplete, resulting in residual $^{1}H-^{1}H$ couplings.[50] The signal refocused was approximately 81% for CTAB and 95% for the CTA cations between titania layers: the percentages were calculated from the intensity of the biggest peak of the last spectrum versus that of the first spectrum in the stacked plots in Figures 9 and 10. The greater refocused signal reflects the smaller $^{13}C-^{1}H$ heteronuclear and residual $^{1}H-^{1}H$ homonuclear couplings, possibly reduced by relatively more molecular motion.[50,51] A 16-point discrete Fourier transform of these signal modulations in the t_1 dipolar dimension yielded 16 sidebands of a dipolar spectrum or pattern in the pure absorption mode for each carbon (4 spectra each at the lower half of Figures 9 and 10). Much broader dipolar linewidths were clearly seen for CTAB (Figure 9) than those for the CTA cations between the titania layers (Figure 10) and the differences of the dipolar patterns between the methyl and methylene groups were more evident. These two observations are consistent with the WISE results, indicating that the dipolar averaging process by molecular motions is more active in the CTA cations between the titania layers than in CTAB compound. The dipolar patterns of C1 and C5−C13 are very similar for CTAB, whereas they are somewhat different for the CTA cations between the titania layers. The ratio among sidebands in DRSE dipolar spectra has been used as an indication of the degree of molecular motion involving the C−H bond vector.[51] In Figure 10, the ratio of the second sideband to the centerband (n_2/n_0) is smaller for the C5−C13 sites (0.37) than for the C1 site (0.51). All of the methylene carbons have the same number, two, of directly bonded protons. Therefore, this small difference in the ratios may be ascribed mainly to the fact that the C5−C13 sites are more mobile than the C1 site even though a single peak represents for C5−C13. This motional difference between C1 and C5−C13 in the cetyl chains results from the fact that the head group and C1 are bound to the surface of the layer, as described above. However, even in the case C1 itself is not bound to the surface, in general, the anisotropic motions of the surfactant are progressively enhanced toward the chain end from the polar head groups strongly interacting with the inorganic framework, as observed in similar chemical systems.[40−42] Our observation of the chemical shift of 33 ppm and the dynamic property for the middle methylene carbons in the cetyl chains between the titania layers is very similar to the previous finding[39,42,44,45] that a well-ordered trans conformation with a 33 ppm chemical shift does not necessarily indicate high rigidity and that the carbons can undergo rotation about the chain axes.

^{13}C signals (∼10%) of oxalates near 168 ppm (not shown) appeared in the ^{13}C SP MAS spectra of the lamellar titania sample, indicating an approximately 1:1 mole ratio of oxalate to CTA cation. Therefore, we cannot rule out the possibility that the oxalates exist as ligands to the surface Ti of titania layers and that the CTA cations interact with the oxygens in these oxalates rather than with dangling oxygen anions

bonded to Ti. The oxalate carbons on the surface titania layers would facilitate the drawing methylene carbons of cetyl chains to the titania surface. This model also agrees with our observation of bent cetyl chains. N−N distances in CTAB are 5.64 and 7.26 Å.[54] More molecular motions of the cetyl chains between the titania layers than in CTAB suggests longer N−N distances for the CTA cations intercalated between the titania layers or relatively more positional flexibility of the head groups. Although the localized negative charges of bromines in CTAB fix the positions of CTA cations, the less-localized negative charge of the titania might result in microscopic heterogeneity and/or more flexibility of the positions of the head groups.

Conclusion

A new synthetic route for the titania mesostructures with ammonium titanyl carboxylates dissolved in basic aqueous solution is presented. Lamellar or mesoporous titania was synthesized according to the size of a carboxylate (i.e., oxalate or citrate) group of a Ti precursor with CTAB ionic templates. ^{13}C SP MAS, WISE, and DRSE spectra revealed that the CTA cations between the titania layers have (1) bent conformations near the head group, (2) rotation of the methylene carbons in trans conformation about the chain axes, (3) ubiquitous rapid rotation of methyl groups, and (4) interdigitated bilayer structures with C15 located close to C5 of the neighbor chains. Such structure and dynamics of the CTA cations between the titania layers results in smaller interlayer space than the full length of a CTA cation in trans conformation (∼2 nm). Some microscopic structural heterogeneity of the CTA cations between the titania layers was detected by split peaks for some individual carbons; however, no clear phase segregation of the CTA cations was observed with regard to structural or molecular dynamics. The ^{15}N NMR data also supports the conclusion that the CTA cations between the titania layers were, and are, in a single phase. The overall higher mobility of the CTA cations between titania layers than in CTAB was explained by wider chain distances or less strong positional fixation of the ammonium head groups due to delocalization of negative charges of titania. As suggested by a referee, solid-state NMR experiments such as nuclear distance measurements accompanying ^{15}N and/or ^{13}C isotope enrichment, to be carried out in near future, would provide additional information on the structures and dynamics of the CTA cations between the titania layers as well as the location of oxalates in the lamellar titania. We are now examining this new lamellar titania for the purpose of host material in the intercalation chemistry.

Acknowledgment. This work was supported by a grant (R01-2003-000-10667-0) from the KOSEF. Sunha Kim and Seen Ae Chae at the KBSI are gratefully acknowledged for some preliminary solid-state NMR experiments and the solution NMR experiment, respectively.

Supporting Information Available: Figure S1 for the ^{15}N CP MAS NMR spectra of the CTA cations between the titania layers and CTAB and Figure S2 for the comparison of the ^{13}C SP and CP MAS NMR spectra of the CTA cations between the titania layers and CTAB (PDF). These materials are available free of charge via the Internet at http://pubs.acs.org.

CM062916W